Supporting Information

The Tunable Effect of Nitrogen and Boron Dopants on Single Walled Carbon Nanotube Support on the Catalytic Properties of Single Gold Atom Catalyst. A First Principles Study of CO Oxidation†

Sajjad Ali,[†,‡] Tianfu Liu,[†,§] Zan Lian,[†,§] Bo Li[,†] and Dang Sheng Su*[,†]*

[†]*Shenyang National Laboratory for Materials Science, Institute of Metal Research, Chinese Academy of Sciences 72 Wenhua Road, Shenyang 110016, China*

[‡]*University of Chinese Academy of Sciences 19 A Yuquan Road, Shijingshan District, Beijing 100049, China*

[§]*School of Materials Science and Engineering, University of Science and Technology of China, Shenyang 110016, China*

Table S1. Binding energy, E_b and Bader charge, Q calculated for the most stable configurations of O_2 and CO and CO-O_2 adsorbed on a SWCNT supported Au atom. Here (c) represents that the adsorption site for Au is Carbon atom.

System CNT	**Au**		**O_2**		**CO**		**CO-O_2**
	E_b(eV)	Q (|e|)	E_b(eV)	Q (|e|)	E_b(eV)	Q (|e|)	E_b(eV)
Axial 55(80) N-CNT	-1.71 (-1.79)	+0.9	-0.29 (1.14)	+0.52	-1.06 (-1.04)	+0.54	-0.85 (-1.03)
Axial 55(80) B-CNT	-2.11 (-1.96)	-0.44	-0.96 (-1.45)	-0.25	-0.703 (-1.14) (c) -0.20 (-0.36)	-0.004	-0.99 (-1.53) (c) -0.93 (-0.91)
Graphitic 55(80)N-CNT	-0.65 (-0.70)	-0.17	-0.34 (-0.36)		-0.08 (-0.93) (c) -0.91 (-0.95)		-0.58 (-0.75)
Graphitic 55(80) B-CNT	-0.907 (-1.35)	-0.20	-0.54(-0.39) (c) -0.63 (-0.39)		-1.01 (-1.11)		-0.68 (-0.27)
Azide 55(80) N-CNT	-0.001 (-0.61)	-0.17	-1.69 (-0.88) (c) -0.50 (-0.38)		-0.92 (-0.94) (c) -0.89 (-0.89)		-1.93 (-0.71)
Azide 55(80) B-CNT	-2.163 (-2.14)	-0.18	-0.51 (-0.45)		-1.15 (-1.05)		-1.16 (-0.44) (c) 0.25 (0.24)
Para 55(80) N-CNT	-0.678 (-0.56)	-0.19	-0.42 (-0.54) (c) -0.52 (-0.57)		-0.21 (-0.95) (c) -0.79 (-0.94)		-0.50 (-0.96)
Para 55(80) B-CNT	-1.108 (-1.32)	-0.17	-0.29(-0.28)		-1.11 (-1.6) (c) -0.96 (-1.07)		-1.04 (-1.13) (c) -1.01 (-0.51)
Meta 55(80) N-CNT	-1.17 (-0.92)	-0.13	-0.55 (-0.66) (c) -0.67 (-0.76)		-1.09 (-1.16)		-0.51 (-0.51)
Meta 55(80) B-CNT	-1.237 (-1.25)	+0.04	-0.72 (-0.7) (c) -0.78 (-0.59)		-1.64 (-1.6) (c) -1.0 (-1.54)		-1.4 (-1.54) (c) -0.81 (-1.51)
Pyridine55 N-CNT	-0.487	+0.41	-1.1	+0.52	-2.6	+0.5	-1.94
Pyridine55 B-CNT	-1.775	-0.55	-1.73	-0.27	-1.25	-0.3	-1.09
Pristine SWCNT (5,5) and (8,0)	-0.38 (-0.36)	-0.08(-0.09)	-0.06(-0.69)	+0.19	-0.99(-1.03)	+0.22	-0.98

Table S2 Comparison of the energy barriers for CO oxidation obtained with different catalysts		
Catalyst	Energy barrier (eV)	Ref.
Au-SWCNT	0.02-0.2[LH], 0.03-0.93[ER],	Present work
Fe-graphyne	0.21 [ER]	[1]
Fe-graphene	0.58 [ER]	[2]
Fe-graphene oxide	0.86 [ER]	[3]
Fe-BN sheet	0.56 to 0.61[ER]	[4]
Au-graphene	0.31 [LH],0.18 [ER]	[5]
Co-graphene	1.33 [ER]	[6]
Co-BN sheet	0.52 [ER]	[7]
Co-phthalocyanine	1.23 [ER], 0.65[LH]	[6]
Pt/Ti-phthalocyanine	0.55 [ER]	[8]
Cu-graphene	0.54 [ER], 0.25 [LH]	[9]
Pt/SWBN	0.24 [ER], 0.37 [LH]	[10]
Au/rutile TiO_2 (110)	0.31 [Mars-van Krevelen mechanism]	[11]
Au/h-BN, Au/V_B @h-BN and Au/V_N @h-BN	0.98 [ER], 0.49[ER], 0.58 [ER]	[12]
Au13 @CeO_2 –STO, Au13 @CeO_2 –3VAC	0.14, 0.33[M-vK mechanism]	[13]
Al-g-ZnO	0.79 [ER]	[14]
Au/HBN	0.09 [TER], 0.46 [BER], 0.39(BLH)	[15]
Pt/SV-graphene	0.58[LH], 0.59 ER	[16]
$CaPt_x Ti_{1-x}O_3$	0.20–0.45	[17]

From the comparison of the energy barriers for CO oxidation obtained with different catalysts it is concluded that the energy barrier is very lower in Conventional B-LH and B-ER mechanism as well as in Tri-ER mechanism.

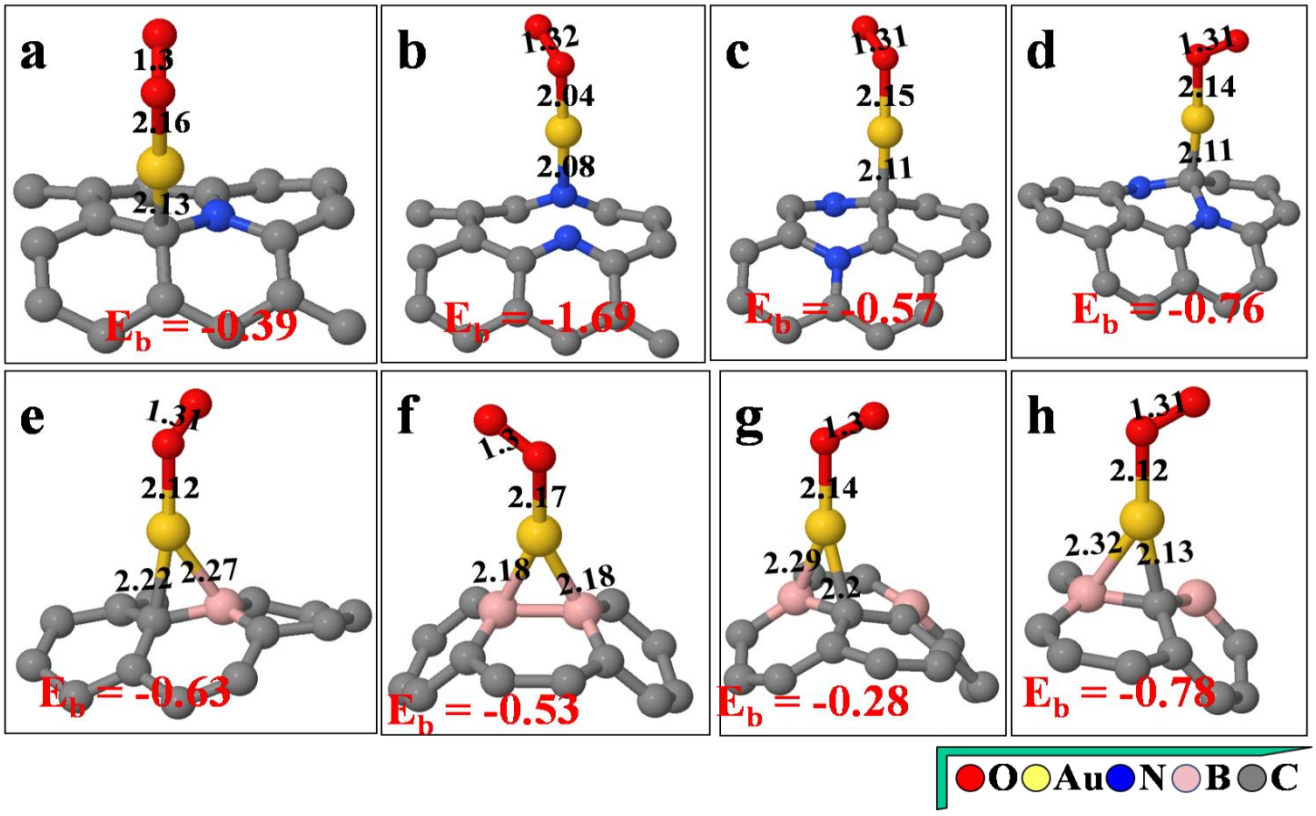

Figure S1. O_2 adsorption on doped SWCNTs with graphitic, azide, Para and Meta, types (a-d) nitrogen and (e-h) boron respectively. E_b represent binding energy in electron volt. The interatomic distances are given in Å. Only a part of SWCNTs are shown.

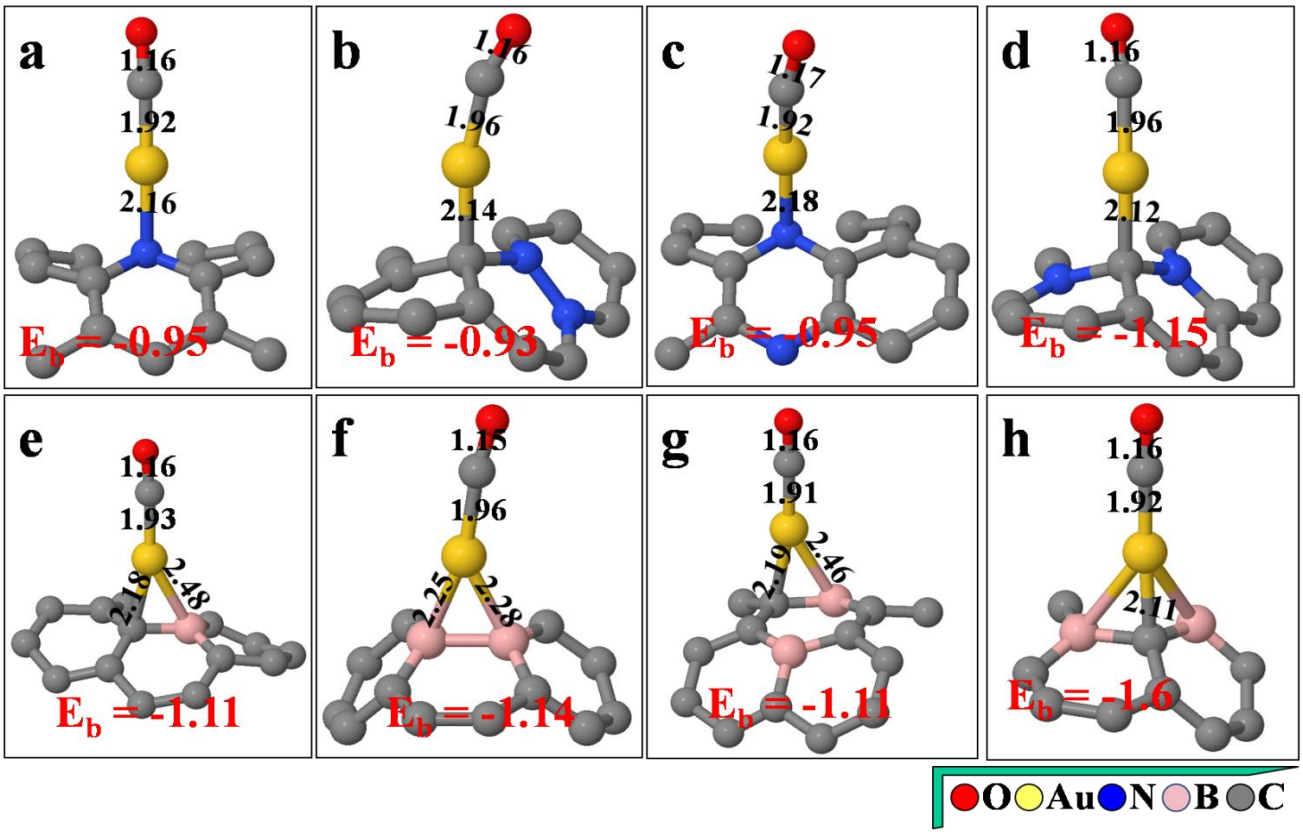

Figure S2. CO adsorption on doped SWCNTs with graphitic, azide, Para and Meta, types (a-d) nitrogen and (e-h) boron respectively. E_b represent binding energy in electron volt. The interatomic distances are given in Å. Only a part of SWCNTs are shown.

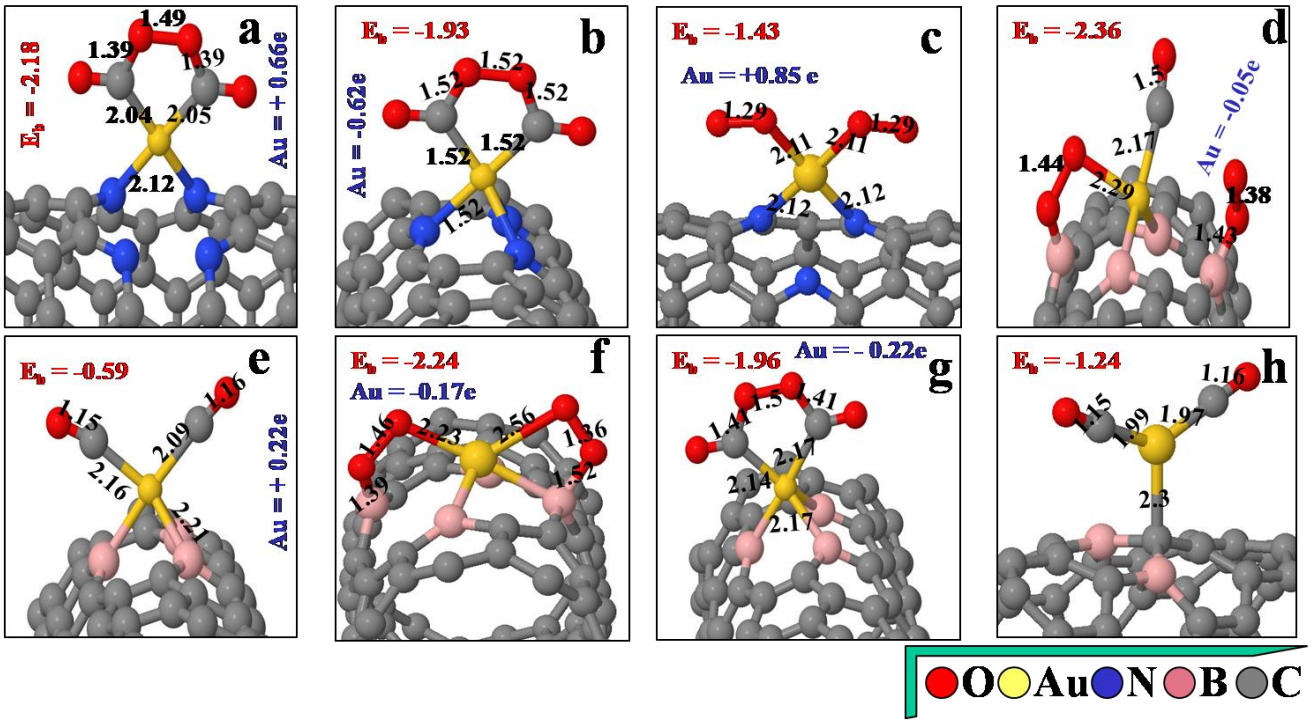

Figure S3. Multiadsorption of 2CO-O_2, $2O_2$, CO-$2O_2$ on doped SWCNTs with pyridine, axial and Meta, types (a-c) nitrogen and (g-h) boron respectively. E_b represent binding energy in electron volt. The interatomic distances are given in Å. Only a part of SWCNTs are shown.

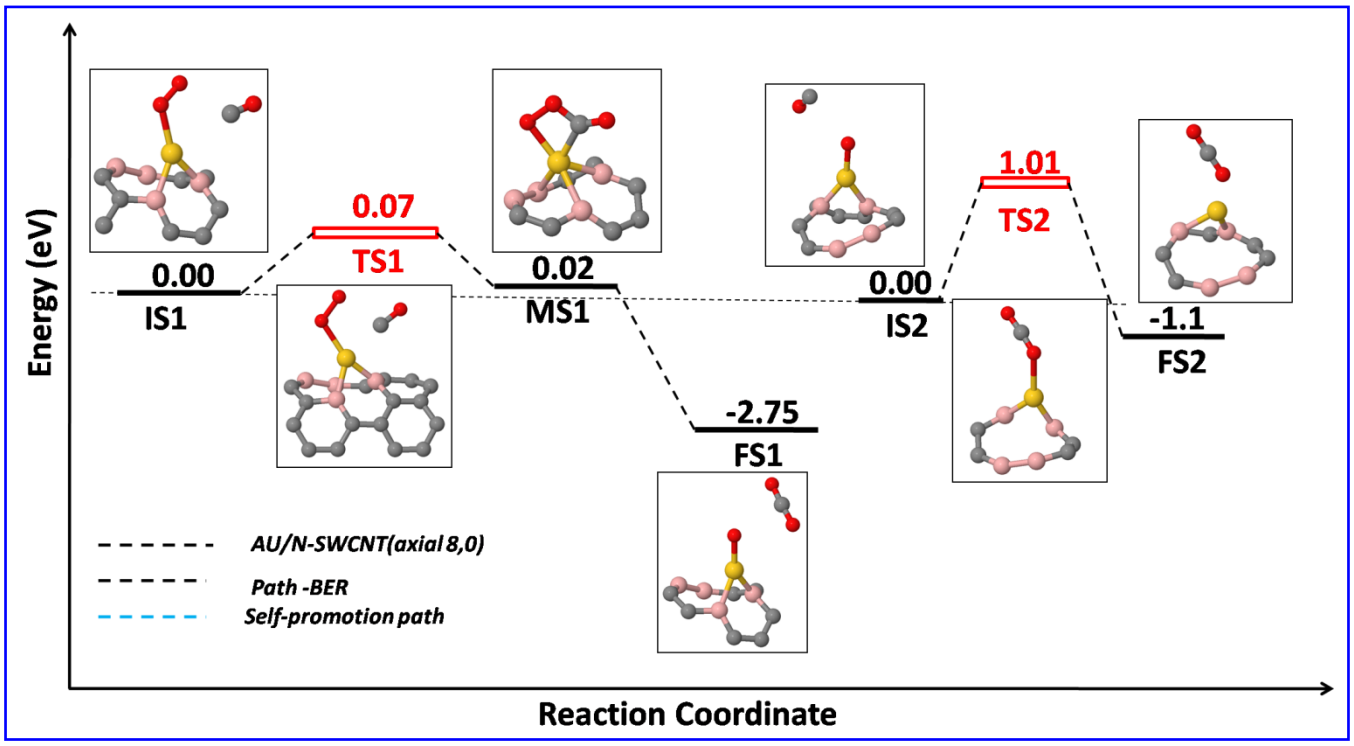

Figure S4. Reaction pathways of CO on Au supported B-SWCNT (axial 8,0). Schematic energy profile corresponding to local configurations along the minimum-energy pathway via the path B-ER. All energies are given with respect to the reference energy, i.e., the sum of energies of the Au/N-SWCNT (8,0 graphitic) and individual CO and O_2 molecules.

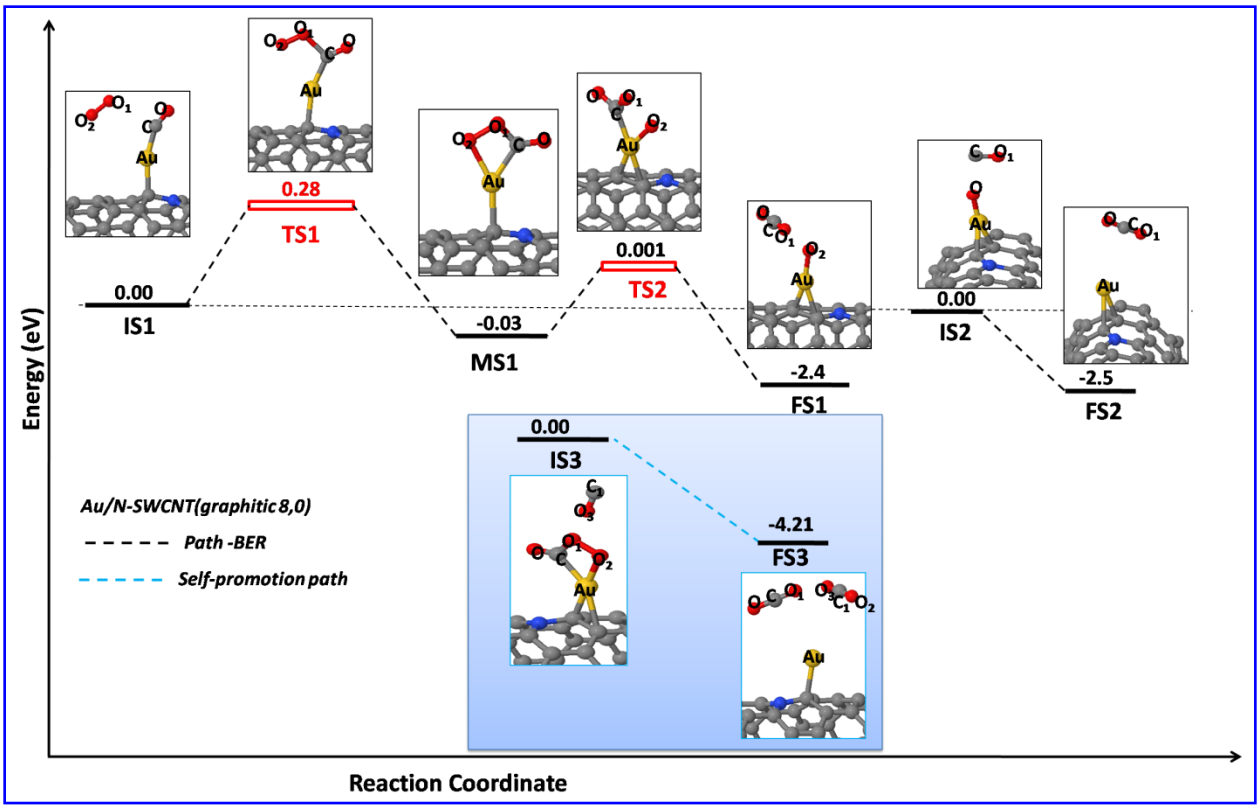

Figure S5. Reaction pathways of CO on Au supported N-SWCNT (8,0 graphitic). Schematic energy profile corresponding to local configurations along the minimum-energy pathway via the path B-ER. All energies are given with respect to the reference energy, i.e., the sum of energies of the Au/N-SWCNT (8,0 graphitic) and individual CO and O_2 molecules.

Table S3. Structural Parameters for the Intermediate States along the Minimum Energy Pathway for the CO Oxidation on the Au/N-SWCNT graphitic (8,0)

(a)	**IS**	**TS**	**MS**	**TS2**
$d_{(O2-O1)}$	1.25	1.3	1.51	1.51
$d_{(C-O)}$	1.16	1.18	1.21	1.22
$d_{(C-Au)}$	1.97	2.02	2.15	2.16
δq [Au]	+0.22	+0.16	+0.33	+3.8
δq [C+O]	1.08+(-1.06) = 0.02	1.14+(-1.12) = 0.02	1.53+(-1.06) = 0.47	1.46+(-1.06) = 0.4
δq $[O_2+O_1]$	-0.06+(-0.07) = -0.12	-0.16+(-0.2) = -0.36	-0.36+(-0.6) = -0.97	-0.6+(-0.4) = -1.02

The units of the bond distance and charge transfer are Å and e respectively. IS, TS, MS and TS are displayed in Figure S5. Charge transfer is calculated using the Bader charge analysis. Negative (positive) δq denotes charge gain (loss).

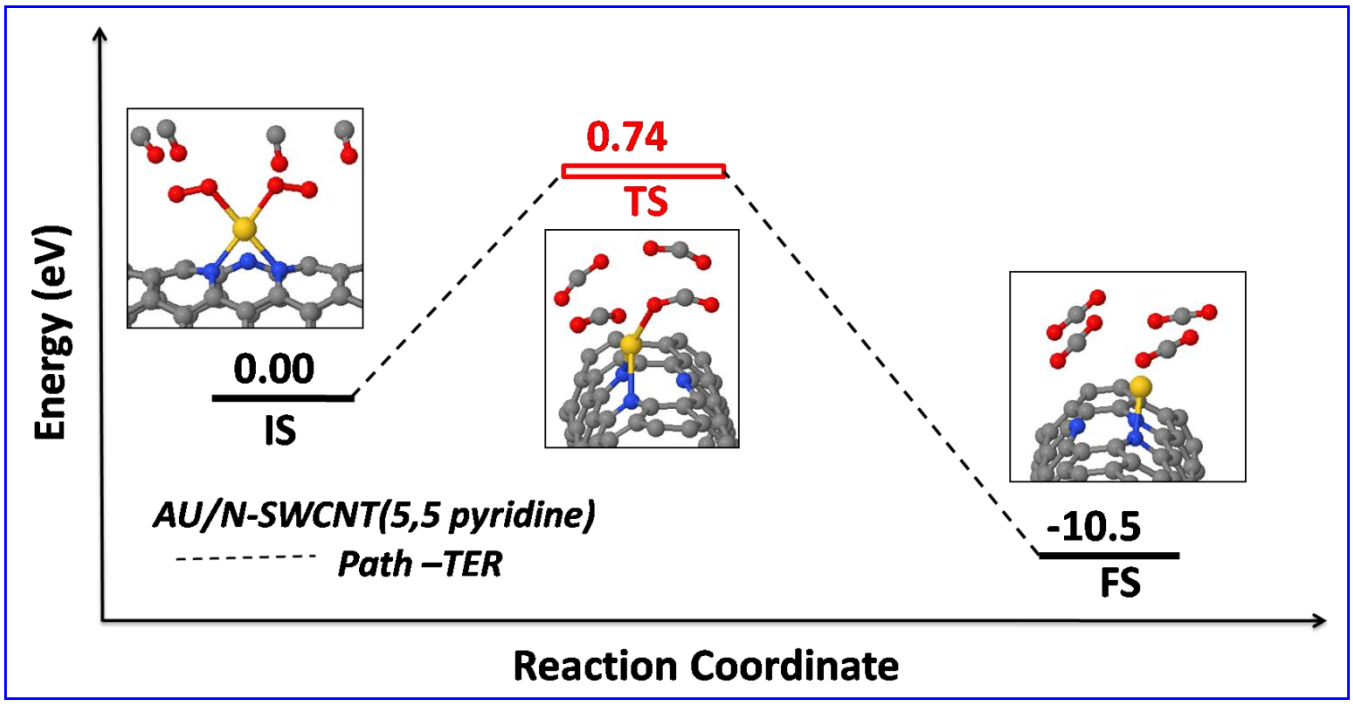

Figure S6. Reaction pathways of CO on Au supported N-SWCNT (5,5 pyridine). CO oxidation follows a hexa-molecular E-R mechanism.

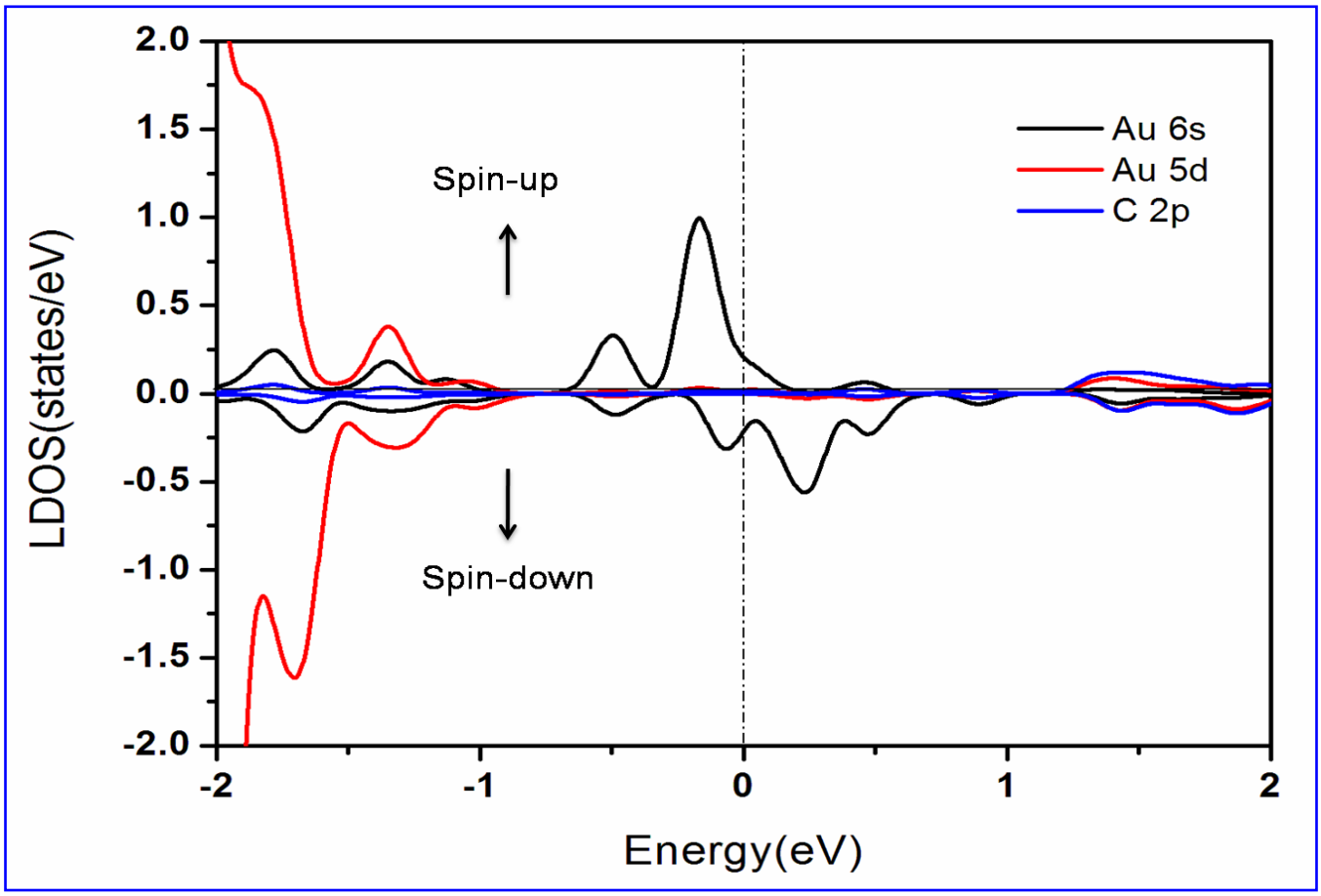

Figure S7. (Color online) The LDOS of Au/SWCNT. Spin-up (↑) and spin-down (↓) states are marked as positive and negative values, respectively. The Fermi level was set to zero.

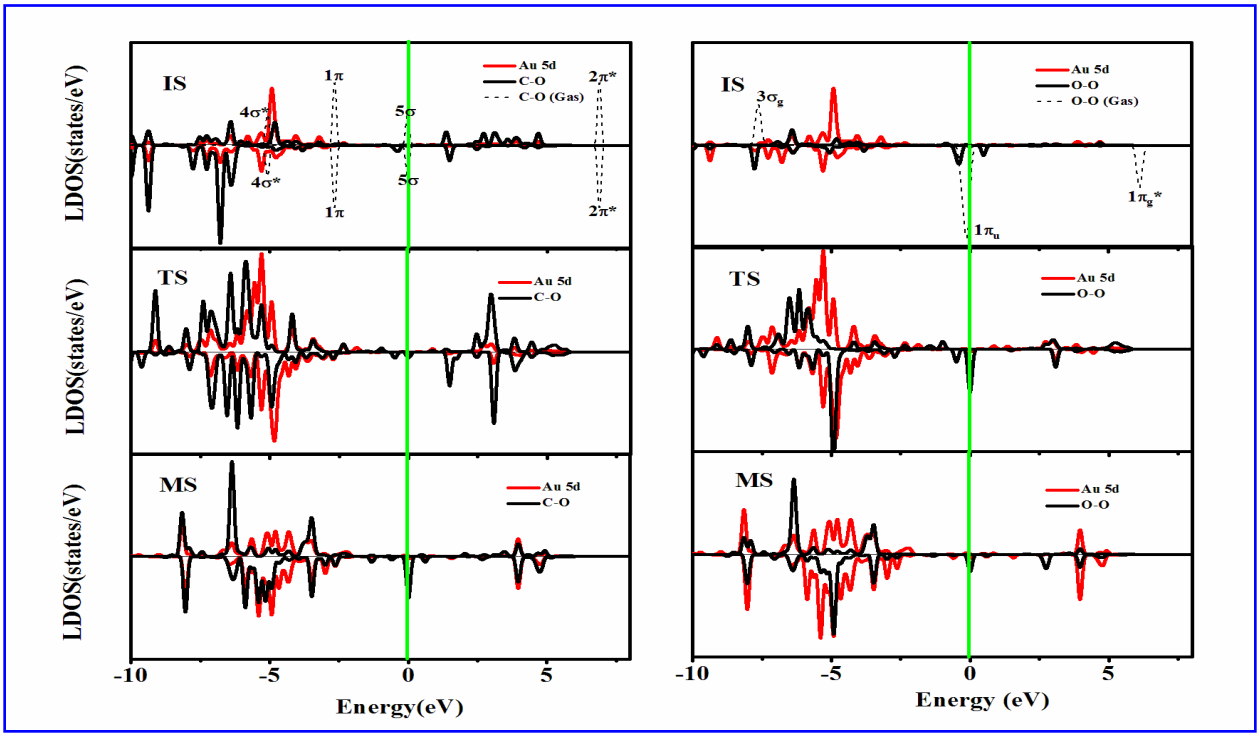

Figure S8. Spin-polarized local density of states (LDOS) projected onto C-O (left panel) and O2-O3 (right panel) on the Au/B-SWCNT pyridine (5,5) (Figure 9a), together with the d-projected LDOS of the Au atom in the IS, TS, and MS. Black dashed curve, gas-phase CO or O_2 ;black solid curve, C-O or O_1-O_2 on Au/B-SWCNT pyridine(5,5); red curve, d-projected LDOS of the Au atom. The Fermi level is set to zero.

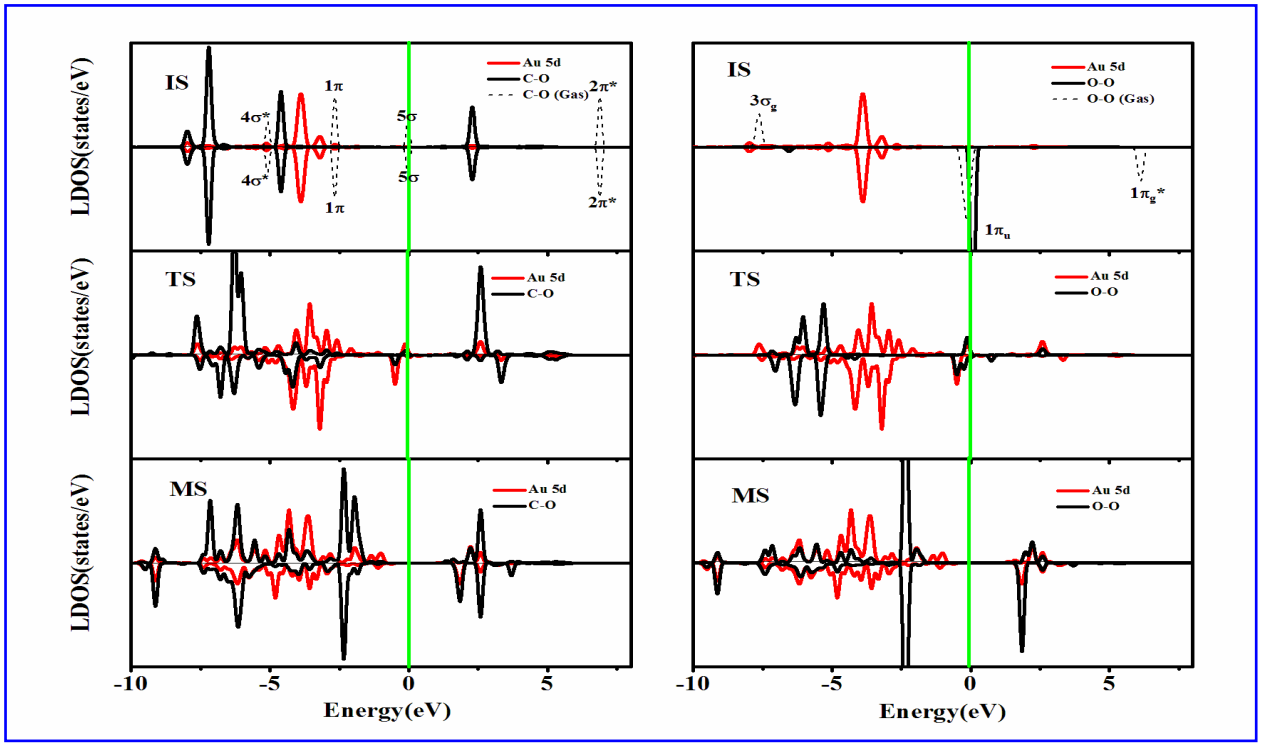

Figure S9. Spin-polarized local density of states (LDOS) projected onto C-O (left panel) and O_2-O_3 (right panel) on the Au/B-SWCNT pyridine (5,5) (Figure 9b), together with the d-projected LDOS of the Au atom in the IS, TS, and MS. Black dashed curve, gas-phase CO

or O_2 ;black solid curve, C-O or O_1-O_2 on Au/B-SWCNT pyridine(5,5); red curve, d-projected LDOS of the Au atom. The Fermi level is set to zero. The spin density is defined as the difference between spin-up and spin-down electron densities, $\rho_\uparrow - \rho_\downarrow$.

Table S4. The effect of diameter (Curvature effect) of SWCNT on the binding energies of Au, CO and O_2 adsorbed on pyridinic nitrogen and boron doped SWCNT.

SWCNT	Diameter(Å)	N-SWCNT		B-SWCNT		N-SWCNT	B-SWCNT	N-SWCNT	B-SWCNT
		Au(E_b)	Q (|e|)	Au(E_b)	Q (|e|)	CO(E_b)	CO(E_b)	O_2(E_b)	O_2(E_b)
(6,0)	4.87	-0.89	+0.23	-1.84	-0.46	-3.06	-2.45	-1.73	-2.41
(8,0)	6.41	-0.88	+0.27	-2.12	-0.43	-3.2	-2.78	-1.71	-2.74
(12,0)	9.55	-0.59	+0.38	-2.06	-0.28	-3.09	-2.85	-1.67	-2.54

References

(1) Wu, P.; Du, P.; Zhang, H.; Cai, C. *Phys. Chem. Chem. Phys.* 2015, *17*, 1441.
(2) Li, Y.; Zhou, Z.; Yu, G.; Chen, W.; Chen, Z. *J. Phys. Chem. C* 2010, *114*, 6250.
(3) Li, F.; Zhao, J.; Chen, Z. *J. Phys. Chem. C* 2012, *116*, 2507.
(4) Zhao, P.; Su, Y.; Zhang, Y.; Li, S.-J.; Chen, G. *Chem. Phys. Lett.* 2011, *515*, 159.
(5) Lu, Y.-H.; Zhou, M.; Zhang, C.; Feng, Y.-P. *J. Phys. Chem. C* 2009, *113*, 20156.
(6) Deng, Q.; Zhao, L.; Gao, X.; Zhang, M.; Luo, Y.; Zhao, Y. *Small* 2013, *9*, 3506.
(7) Lin, S.; Ye, X.; Johnson, R. S.; Guo, H. *J. Phys. Chem. C* 2013, *117*, 17319.
(8) Chen, X. F.; Yan, J. M.; Jiang, Q. *J. Phys. Chem. C* 2014, *118*, 2122.
(9) Song, E. H.; Wen, Z.; Jiang, Q. *J. Phys. Chem. C* 2011, *115*, 3678.
(10) Abdel Aal, S. *Surface Science* 2016, *644*, 1.
(11) Chrétien, S.; Metiu, H. *Catal. Lett* 2006, *107*, 143.
(12) Gao, M.; Lyalin, A.; Taketsugu, T. *J. Chem. Phys.* 2013, *138*, 034701.
(13) Kim, H. Y.; Lee, H. M.; Henkelman, G. *J. Am. Chem. Soc* 2012, *134*, 1560.
(14) Ma, D.; Wang, Q.; Li, T.; Tang, Z.; Yang, G.; He, C.; Lu, Z. *J. Mater. Chem. C.* 2015, *3*, 9964.
(15) Mao, K.; Li, L.; Zhang, W.; Pei, Y.; Zeng, X. C.; Wu, X.; Yang, J. *Sci. Rep.* 2014, *4*, 5441.
(16) Tang, Y.; Yang, Z.; Dai, X. *Physical Chemistry Chemical Physics* 2012, *14*, 16566.
(17) Zhang, Q.; Li, B.; Wang, H.; Suo, Y.; Chen, L. *RSC Adv.* 2014, *4*, 30530.